Differential measurements of jet sub-structure observables and their correlation in p+p collisions at $\sqrt{s} = 200$ GeV in STAR

Monika Robotková for the STAR Collaboration*

Nuclear Physics Institute of the CAS
* robotmon@fjfi.cvut.cz

August 9, 2021

Proceedings for the XXVIII International Workshop on Deep-Inelastic Scattering and Related Subjects, Stony Brook University, New York, USA, 12-16 April 2021
doi:10.21468/SciPostPhysProc.?

Abstract

This analysis extends recent measurements of the jet sub-structure observables based on the SoftDrop algorithm in p+p collisions at $\sqrt{s} = 200$ GeV in the STAR experiment. We present fully unfolded multi-differential measurements of jet sub-structure observables at the first split and their correlations for jets of different transverse momenta and radii. We compare our measurements to various Monte Carlo models.

1 Introduction

Jets are collimated sprays of hadrons that are produced in high energy particle collisions. Jet sub-structure measurements serve as an experimental tool for studying Quantum Chromodynamics (QCD) and parton shower evolution. Evolution of hard scattered partons is described via a shower algorithm based on both momentum and angular scales. In order to better assess the jet sub-structure, it is necessary to use a jet grooming technique such as SoftDrop [1]. This technique connects parton shower and angular tree, and removes soft radiations within a jet. In the SoftDrop framework, when a jet is reconstructed using the anti-k_{T} algorithm [2], it is reclustered with the C/A algorithm [3] to get an angular ordered tree. The jet is then divided into two sub-jets, labeled as 1 and 2, by undoing the last step of the C/A algorithm. If the two sub-jets pass the SoftDrop condition

$$\frac{\min(p_{\mathrm{T},1}, p_{\mathrm{T},2})}{p_{\mathrm{T},1} + p_{\mathrm{T},2}} > z_{\mathrm{cut}} \left(\frac{\Delta R_{1,2}}{R} \right)^{\beta}, \tag{1}$$

then the jet is considered as the final SoftDrop jet. In Eq. 1, $p_{\mathrm{T,i}}$ corresponds to the transverse momentum of the sub-jet, $\Delta R_{1,2}$ is the distance between sub-jets and R is the resolution parameter. If the condition is not met, the sub-jet with the higher p_{T} is denoted as the starting jet and the whole process is repeated until the condition is met. The SoftDrop procedure depends on two parameters, β and z_{cut}, which are set to $\beta = 0$ and $z_{\mathrm{cut}} = 0.1$. The products of this procedure are two jet sub-structure observables, shared momentum fraction (z_{g}) and groomed radius (R_{g}). The shared momentum fraction is defined as $z_{\mathrm{g}} = \frac{\min(p_{\mathrm{T},1}, p_{\mathrm{T},2})}{p_{\mathrm{T},1}+p_{\mathrm{T},2}}$ and the groomed radius is defined as the first $\Delta R_{1,2}$ that satisfies the SoftDrop condition.

In the previous STAR measurements [4], the momentum and angular scales were measured independently via SoftDrop observables, z_{g} and R_{g}, for jets of varying transverse momenta and

resolution parameters. Our goal is to extend previous measurements and study the correlation between the observables z_g and R_g as a function of jet transverse momentum ($p_{T,jet}$). Another way to explore the jet sub-structure is to use the Lund Plane diagram [5]. This theoretical toolkit represents the phase-space of the jet evolution by a 2D triangular plane of the transverse momenta and the angles of emissions with respect to their emitters. Recent ATLAS and ALICE measurements of the Lund Plane [6,7] showed significant differences in the groomed jet radius between models with varying hadronization and parton shower implementations. We explore these differences via SoftDrop observables at lower p_T than LHC measurements, where non-perturbative effects are expected to be larger.

2 Data analysis

Data for this analysis were collected by the STAR experiment [8] in 2012 for p+p collisions at $\sqrt{s} = 200$ GeV. Events are triggered via a 1×1 patch in pseudorapidity×azimuthal angle ($\eta \times \phi$) in the Barrel Electromagnetic Calorimeter (BEMC) [9] with a total transverse energy $E_T > 7.3$ GeV. Jets are reconstructed using charged-particle tracks from the Time Projection Chamber (TPC) [10] and BEMC towers in the range $0.2 < p_T(E_T) < 30$ GeV/c (GeV). Reconstructed charged-particle tracks are matched to BEMC towers and hadronic correction is applied to avoid double counting of charged-particle tracks' energies deposited in the BEMC.

Jets are reconstructed with the anti-k_T algorithm for two values of resolution parameter, $R = 0.4$ and $R = 0.6$. They are required to have $p_{T,jet} > 10$ GeV/c and to lie within the pseudo-rapidity $|\eta_{jet}| < 1.0 - R$ to assure that the jet cone is fully contained in the STAR acceptance.

Since the measurement is affected by finite efficiency and detector resolution, these effects have to be deconvolved to obtain particle-level distributions. These observables lie in 3-dimensional space, ($p_{T,jet}$, z_g, R_g), and thus multi-dimensional unfolding is needed. The 2D unfolding for (z_g, R_g) is done with a response matrix which contains particle-level and detector-level distributions. Particle-level distributions are obtained from the PYTHIA 6 events [11] with the STAR Perugia tune [12]. They are then passed through the GEANT3 detector simulation [13] and embedded into zero-bias events to obtain detector-level distributions. We apply an iterative Bayesian unfolding [14], implemented in the RooUnfold framework [15], on measured 2D (z_g, R_g) distributions in four different detector-level $p_{T,jet}$ intervals, namely, $p^{det}_{T,jet} \in$ [15,20], [20,25], [25,30], and [30,40] GeV/c. Following the removal of the detector effects on the sub-structure observables, the correction for $p_{T,jet}$, due to jet energy scale and resolution effects, is applied as follows. Projections of the detector level jet p_T distributions are obtained from the jet p_T response matrix (Fig. 1 in [4]) for selected particle-level p_T intervals used in this measurement. These projections are then normalized to unity and used as weights to be applied to unfolded z_g vs. R_g distributions, followed by a correction for the jet finding efficiency, resulting in 3D fully corrected measurements in selected particle-level p_T intervals.

Systematic uncertainties on our measurements are estimated from the following sources - tracking efficiency, tower energy scale, hadronic correction and unfolding. These are the same sources which are explored in previous jet sub-structure measurement [4]. The first source of the systematic uncertainty is the hadronic correction, which is evaluated by varying the fraction of track momentum subtracted from the nominal value of 100% to 50%. The precision of the BEMC tower calibration is 3.8% and the uncertainty in the TPC tracking efficiency is 4%. The systematic uncertainty coming from the unfolding method is estimated by varying the iteration parameter from 4 to 6. The systematic uncertainty due to the prior shape variation has not been estimated yet and will be included in the forthcoming publication. An example of the magnitudes of each individual systematic uncertainty and total systematic uncertainty for z_g distributions in three R_g intervals for jets with $R = 0.4$ and $20 < p_{T,jet} < 25$ GeV/c is plotted in

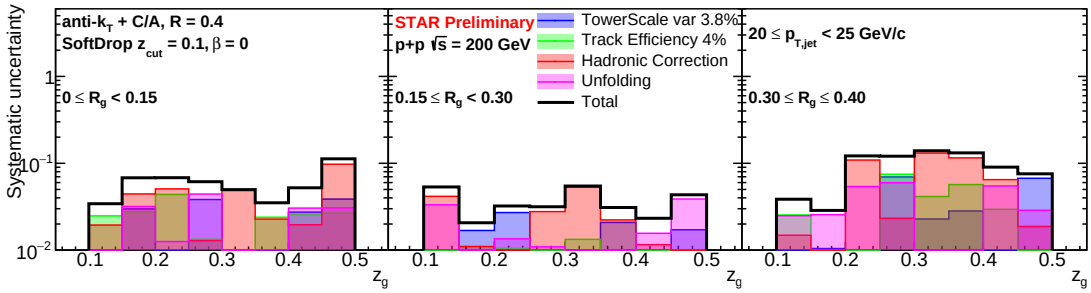

Figure 1: Systematic uncertainties for z_g in three R_g bins for jets with $R = 0.4$ and $20 < p_{T,jet} < 25$ GeV/c.

Fig. 1. The largest contribution comes from the hadronic correction and unfolding. The total uncertainty is typically about 5-10%.

3 Results and Monte Carlo comparisons

Fully unfolded z_g vs. R_g distributions for four different $p_{T,jet}$ intervals and $R = 0.4$ are shown in Fig. 2. Bands around the data points correspond to the total systematic uncertainties discussed in Sec. 2. We observe a significant change to the shape of the z_g distributions as the R_g is varied. Jets with a large R_g tend to have steeper z_g distributions representing an enhanced probability of softer splits as compared to jets with a smaller R_g which consequently have a much flatter z_g due to collinear hard splittings. The dependence on the $p_{T,jet}$ is observed to be small compared to the R_g which essentially determines the shape of the z_g.

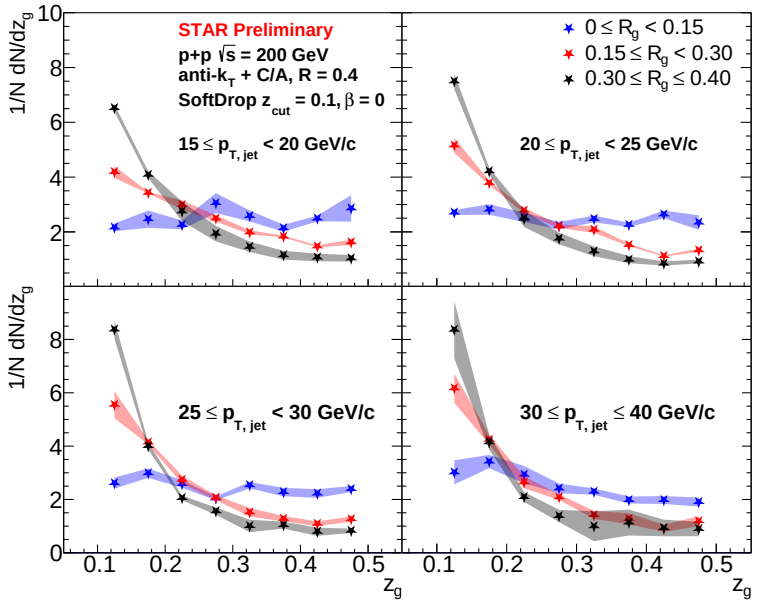

Figure 2: Fully unfolded z_g distributions for three R_g bins for jets with $R = 0.4$ in p+p collisions at $\sqrt{s} = 200$ GeV. Individual panels correspond to different $p_{T,jet}$ intervals (see legend).

In Fig. 3, a comparison of the unfolded z_g vs. R_g distributions for different resolution

parameters, $R = 0.4$ on the left and $R = 0.6$ on the right, is shown. In this case, the distributions are shown only for two R_g bins, $0 < R_g < 0.15$ and $0.15 < R_g < 0.30$. In both cases, the distributions look very similar, which shows that the choice of jet radius does not significantly affect the jet sub-structure.

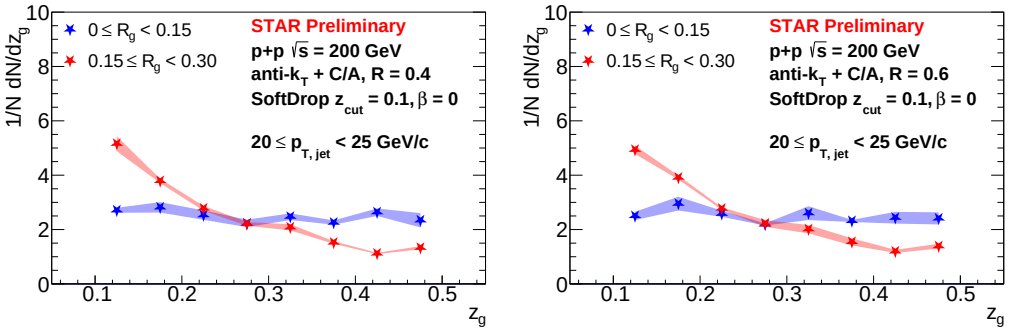

Figure 3: Fully unfolded z_g distributions in two R_g bins for jets with $20 < p_{T,jet} < 25$ GeV/c and $R = 0.4$ (left) or $R = 0.6$ (right).

The fully corrected z_g distributions are compared with several Monte Carlo (MC) models, such as PYTHIA 6 with Perugia 2012 tune, PYTHIA 8 [16] with the Monash tune based on LHC data [17] and HERWIG 7 [18] with the EE5C underlying event tune [19]. There are differences in parton shower implementations in these MC generators. In HERWIG, the parton shower is angularly ordered whereas both PYTHIA versions employ k_T/p_T ordering. There are also differences in the hadronization models, i. e. PYTHIA uses the Lund string model whereas HERWIG is based on the cluster model.

The comparison of z_g distributions in three different R_g bins for jets with $R = 0.4$ and $20 < p_{T,jet} < 25$ GeV/c between data and MC simulations is displayed in Fig. 4. All of the MC models describe the trend observed in data. There are slight differences between the models especially for the most narrow splittings which will be followed up to disentangle the impact of perturbative and non-perturbavite QCD effects.

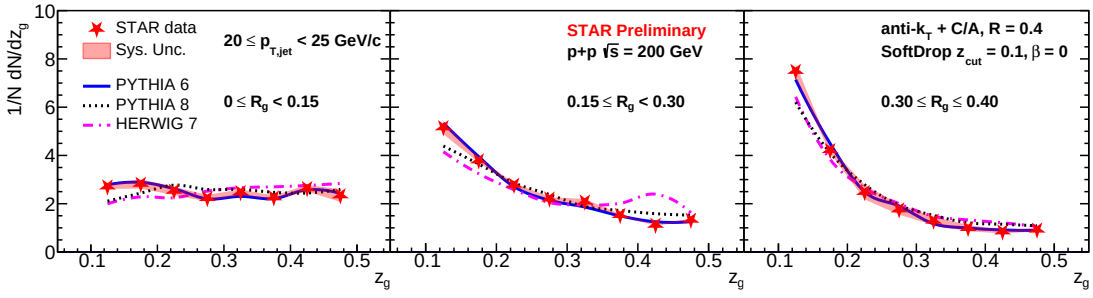

Figure 4: Fully unfolded z_g distributions in three R_g bins for jets with $R = 0.4$ and $20 < p_{T,jet} < 25$ GeV/c in p+p collisions at $\sqrt{s} = 200$ GeV, compared with Monte Carlo simulations.

4 Conclusion

We presented the first measurement of correlations between jet sub-structure observables z_g vs. R_g in different $p_{T,jet}$ intervals utilizing the 2+1D unfolding method. z_g distributions show a

strong dependence on R_g and weak dependence on $p_{T,jet}$, which allows us to isolate soft splits by selecting wide angle splits. The distributions are compared with Monte Carlo simulations, all of which capture the trend observed in data. The next steps of our analysis will focus on disentangling perturbative and non-perturbative QCD effects in the MC simulations and extending to comparisons with theoretical calculations.

References

[1] A. J. Larkoski, S. Marzani, G. Soyez and J. Thaler, *Soft Drop*, Journal of High Energy Physics **2014**(5) (2014), doi:10.1007/JHEP05(2014)146.

[2] M. Cacciari, G. P. Salam and G. Soyez, *The anti-k_t jet clustering algorithm*, Journal of High Energy Physics **2008**(04), 063 (2008), doi:10.1088/1126-6708/2008/04/063.

[3] *A Cambridge-Aachen (C-A) based Jet Algorithm for boosted top-jet tagging* (2009).

[4] J. Adam et al., *Measurement of Groomed Jet Substructure Observables in p+p Collisions at $\sqrt{s_{NN}}$= 200 GeV with STAR*, Physics Letters B **811**, 135846 (2020), doi:https://doi.org/10.1016/j.physletb.2020.135846.

[5] F. A. Dreyer, G. P. Salam and G. Soyez, *The Lund jet plane*, Journal of High Energy Physics **2018**(12) (2018), doi:10.1007/JHEP12(2018)064.

[6] G. Aad et al., *Measurement of the Lund Jet Plane Using Charged Particles in 13 TeV Proton-Proton Collisions with the ATLAS Detector*, Physical Review Letters **124**(22), 222002 (2020), doi:10.1103/PhysRevLett.124.222002.

[7] L. Havener, *Jet splitting measurements in Pb–Pb and pp collisions at $\sqrt{s_{NN}} = 5.02$ TeV with ALICE*, Nuclear Physics A **1005** (2021), doi:10.1016/j.nuclphysa.2020.121906.

[8] K.H. Ackermann et al., *Star detector overview*, Nuclear Instruments and Methods in Physics Research Section A: Accelerators, Spectrometers, Detectors and Associated Equipment **499**(2), 624 (2003), doi:https://doi.org/10.1016/S0168-9002(02)01960-5.

[9] T. M. Cormier et al., *STAR barrel electromagnetic calorimeter absolute calibration using "minimum ionizing particles" from collisions at RHIC*, Nuclear Instruments and Methods in Physics Research Section A: Accelerators, Spectrometers, Detectors and Associated Equipment **483**(3), 734 (2002), doi:10.1016/S0168-9002(01)01951-9.

[10] M. Anderson et al., *The STAR time projection chamber*, Nuclear Instruments and Methods in Physics Research Section A: Accelerators, Spectrometers, Detectors and Associated Equipment **499**(2-3), 659 (2003), doi:10.1016/S0168-9002(02)01964-2.

[11] T. Sjöstrand, S. Mrenna and P. Skands, *PYTHIA 6.4 physics and manual*, Journal of High Energy Physics **2006**(05), 026 (2006-05-01), doi:10.1088/1126-6708/2006/05/026.

[12] P. Z. Skands, *Tuning Monte Carlo generators*, Physical Review D **82**(7) (2010), doi:10.1103/PhysRevD.82.074018.

[13] R. Brun, R. Hagelberg, M. Hansroul and J. C. Lassalle, *Geant: Simulation Program for Particle Physics Experiments. User Guide and Reference Manual* (1978).

[14] G. D'Agostini, *A multidimensional unfolding method based on bayes' theorem*, Nuclear Instruments and Methods in Physics Research Section A: Accelerators, Spectrometers, Detectors and Associated Equipment **362**(2-3), 487 (1995), doi:10.1016/0168-9002(95)00274-X.

[15] T. Adye, *Unfolding algorithms and tests using RooUnfold*, In *PHYSTAT 2011*. CERN, Geneva, doi:10.5170/CERN-2011-006.313 (2011), 1105.1160.

[16] T. S. et al., *An introduction to PYTHIA 8.2*, Computer Physics Communications **191**, 159 (2015), doi:10.1016/j.cpc.2015.01.024.

[17] P. Skands, S. Carrazza and J. Rojo, *Tuning PYTHIA 8.1*, The European Physical Journal C **74**(8) (2014), doi:10.1140/epjc/s10052-014-3024-y.

[18] J. Bellm et al., *Herwig 7.0/Herwig++ 3.0 release note*, The European Physical Journal C **76**(4) (2016), doi:10.1140/epjc/s10052-016-4018-8.

[19] M. Seymour and A. Siodmok, *Constraining MPI models using eff and recent Tevatron and LHC Underlying Event data*, Journal of High Energy Physics **2013** (2013), doi:10.1007/JHEP10(2013)113.